Nuclear Instruments and Methods in Physics Research B 82 (1993) 503–512
North-Holland

NIM B
Beam Interactions with Materials & Atoms

# Incorporation of single elastic scattering in the EGS4 Monte Carlo code system: tests of Molière theory

Alex F. Bielajew and Ruqing Wang
*Institute for National Measurement Standards, National Research Council of Canada, Ottawa K1A 0R6, Canada*

Simon Duane
*National Physical Laboratory, Teddington, UK*

Received 15 January 1993 and in revised form 16 March 1993

To avoid prohibitively long computation times, conventional Monte Carlo $e^-$ transport algorithms (e.g. EGS4, ETRAN, ITS) employ multiple scattering theories and "condensed history" methods to model $e^-$ transport. Although highly successful for many calculations, these techniques do not model backscatter very well, particularly for high-$Z$ materials. In an attempt to correct for this shortcoming, we have extended the EGS4 Monte Carlo code to allow for the simulation of single elastic scattering. The single scattering method also allows quantities to be scored in submicrometer dimension geometries where the Molière multiple scattering theory fails and the Goudsmit–Saunderson multiple scattering equations converge very slowly. Two single scattering schemes have been implemented: (i) Screened Rutherford cross sections which form the basis of Molière's multiple scattering theory, (ii) Single scattering cross sections based upon phase-shift data. In this work we describe the implementation of single elastic scattering in the EGS4 Monte Carlo code system and employ it to verify the Molière multiple scattering theory in its range of validity. We demonstrate that the Molière multiple scattering formalism provides a good description of multiple scattering despite its use of a relatively crude cross section and that it may be employed with semi-quantitative accuracy in the plural scattering regime, where electron step-lengths are so short that only as few as five atoms participate in the angular deflection. However, the remaining differences of the Molière distributions with the phase-shift data motivate the use of more accurate fundamental data, in particular, for applications involving high-$Z$ elements.

## 1. Introduction – why single scattering?

In the realm of coupled electron–photon Monte Carlo transport codes applicable at energies above 10 keV, there are two general-purpose codes enjoying wide-spread use. The EGS code system [1] and the ETRAN[#1] code [4] are based on Berger's "condensed-history" technique [5], whereby single electron elastic and inelastic scatterings are gathered using statistical theories that express the energy loss and deflection angles at the end of electron steps of a fixed or variable length. This effects a considerable reduction in the time required to compute the slowing down of an electron, but it introduces approximations.

Recently, more sophisticated approaches to electron transport have been attempted, PRESTA in the case of EGS [6] and TLC in the case of ETRAN [4]. (The elements of the TLC algorithm were spelled out in Berger's original paper [5].) Although there appears to be much improvement in the stability of electron transport calculations using these new methods, backscatter is still unstable (but less so) with respect to parameters that control the amount of energy loss per electron step. It is unsatisfactory that results depend upon transport parameters that are arbitrary in their choice.

Thus, we are motivated to include single scattering for two principal reasons:

(i) To allow backscatter-dependent problems to be calculated with greater accuracy and less ambiguity.

(ii) To serve as a theoretical laboratory for further research into making the condensed-history technique more accurate.

Condensed history techniques, since they can use orders of magnitude less time than single scattering techniques, will continue their wide-spread use, particularly if the backscattering problem can be eliminated. One recent approach, the "response history method" [7] condenses many single collisions into distributions encompassing many collisions – similar to the condensed history approach but with fewer as-

*Correspondence to*: A.F. Bielajew, Institute for National Measurement Standards, National Research Council of Canada, Ottawa K1A 0R6, Canada.

[#1] In this report, ETRAN stands for the original code plus its spinoffs, ITS [2] and MCNP4 [3].

Elsevier Science Publishers B.V.

sumptions. The incorporation of the response history method in a general-purpose Monte Carlo approach has yet to be done, although being contemplated in the All Particle Method, a Monte Carlo code under development at the Lawrence Livermore National Laboratory [8,9].

In this report we discuss progress towards the implementation of single elastic scattering in the EGS code. The implementation of the phase-shift cross sections is incomplete at this stage and presently works only for elemental materials in the energy range 1–1024 keV. The single elastic scattering cross sections are based upon a partial-wave analysis of the relativistic Dirac equation as developed by Riley et al. [10] but extended from 1 to 1024 keV. The static Coulomb potentials were obtained using the code of Desclaux [11]. This work is described elsewhere [12] and is subject to some limitations in its low-energy range. However, it is the most accurate elastic electron cross section database available[#2]. At the present level of development, inelastic collisions below the energy creation threshold in the EGS4 code are still modeled using the CSDA approximation. It has been shown [7] that for complete accuracy in the calculation of energy spectra, inelastic collisions should be modeled individually. This extension to the EGS4 Monte Carlo system is left for future work.

## 2. Incorporation of single scattering into the EGS4 code system

This section summarises the effort to incorporate single elastic scattering into the EGS4 code system. Much of the detail is documented elsewhere [13,14].

An independent computer program was set up to calculate the cubic spline coefficients for the mean free path and tables of cumulative probability for the sampling of angular distributions from the phase-shift cross sections. This program is executed prior to simulations similar to the data preparation program PEGS4, part of the EGS4 code system. At present, the single scattering model allows only for the use of pure atomic materials.

The screened Rutherford cross section requires data that is intrinsic to the EGS4 system. However, several adjustments to the parametrisation were made to make it consistent with the definitions given by Berger [12]. In particular, an EGS4 high-energy approximation to the screening angle, $\chi_\alpha$, was corrected[#3].

Four new subroutines are linked to the EGS4 system. For sampling phase-shift cross sections, SSDIST samples randomly the drift distance to a point of elastic scattering and SSANG samples the deflection angle. The screened Rutherford cross sections have two analogous subroutines named SSDIST_SR and SSANG_SR. The screened Rutherford angular distribution, having the form $dP(\Theta) = \sin\Theta\, d\Theta(\chi_\alpha^2/4)[2 + \chi_\alpha^2/2](1 - \cos\Theta + \chi_\alpha^2/2)^{-2}$, was sampled analytically using the direct inversion technique.

Several changes were made to the EGS4 subroutine ELECTR, which executes electron transport. Effectively, the additions convert the multiple scattering substeps into repeated single scattering events with drift distances between elastic scatterings and deflections at the elastic scattering loci. The parameter TMXS, which controls the maximum electron step-size of a multiple scattering substep was set to infinity. The curved path, TUSTEP, of a multiple scattering substep is set equal to the straight geometrical path, USTEP. USTEP represents an accumulation of drift distances between elastic scatterings. Finally, scattering was turned off when a transport step was interrupted by the crossing of a material boundary or the interface between two geometrical elements.

In addition, single scattering or Molière multiple scattering can be enabled on a region-by-region basis within the code. Moreover, the capability of turning off all energy loss processes was incorporated to isolate the comparison to only elastic scattering processes.

## 3. Comparison of single and multiple scattering

### 3.1. Single scattering cross sections

The Molière multiple scattering theory [15,16] is developed using the screened Rutherford cross section. The inclusion of this cross section is done at an early stage of the mathematical development and is inherent in the subsequent mathematical expressions[#4].

[#2] The authors are grateful to Dr. Martin J. Berger of NIST for making the ELAST database available to us in advance of general distribution.

[#3] Molière's screening angle is given conventionally as $\chi_\alpha^2 = 6.8 \times 10^{-5} Z^{2/3}(\tau(\tau + 2))^{-1}[1.13 + 3.76(Z/137\beta)^2]$, in the notation of Berger [12]. In the EGS4 implementation, the $\beta$ is approximated as unity. This generally has very little effect except at very low energy.

[#4] While this may seem like a disadvantage, the inclusion of the cross section at an early stage allows the mathematical development to proceed and allows a material-independent form of the equations to be expressed. It is difficult to change the angular dependence of the single scattering cross section input to the Molière formalism without altering the mathematics drastically.

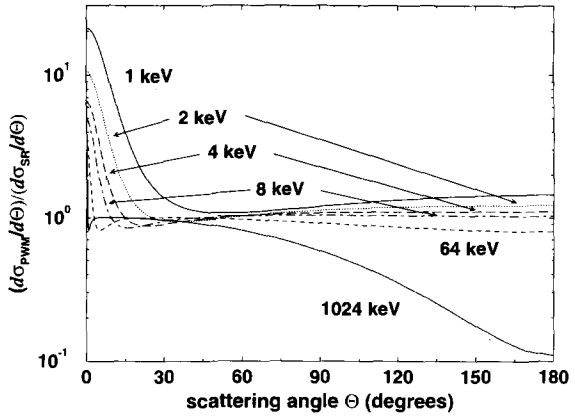


Fig. 1. The ratio of the differential cross section using the partial-wave method to the screened Rutherford cross section for graphite at energies 1, 2, 4, 8, 64, and 1024 keV.

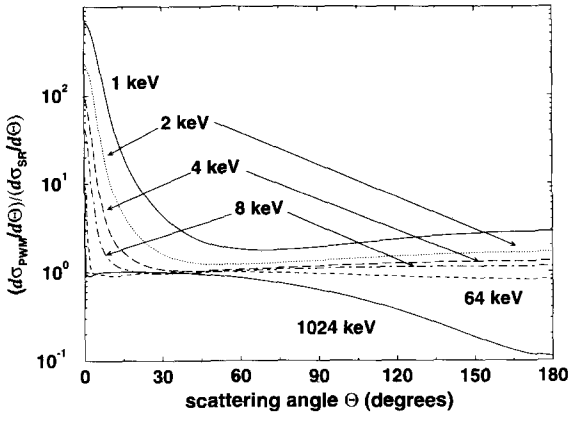


Fig. 2. The ratio of the differential cross section using the partial-wave method to the screened Rutherford cross section for aluminium at energies 1, 2, 4, 8, 64, and 1024 keV.

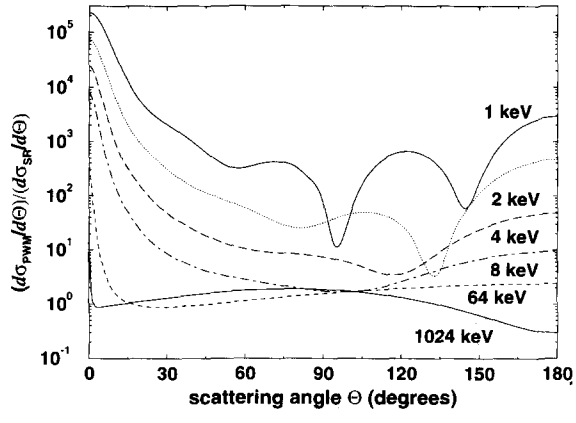


Fig. 3. The ratio of the differential cross section using the partial-wave method to the screened Rutherford cross section for gold at energies 1, 2, 4, 8, 64, and 1024 keV.

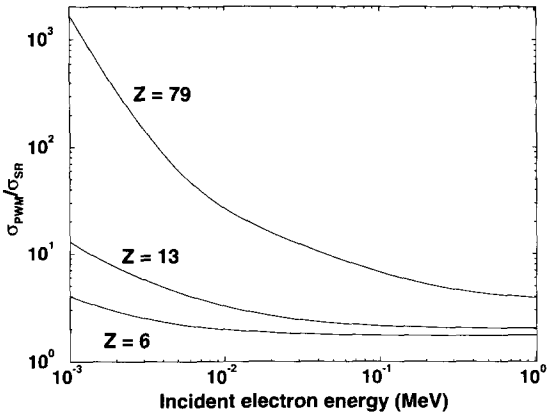


Fig. 4. The ratio of the total cross section using the partial-wave method to the screened Rutherford cross section for graphite, aluminium, and gold from 1 to 1024 keV.

Thus it is appropriate to compare the single scattering cross sections, since the differences will also carry on to the multiple scattering distributions which involve further approximations.

To this end, we have compared the ratios of the differential cross sections obtained using the partial-wave method (PWM) to the screened Rutherford cross section as employed in the Molière theory and plotted the results for graphite, aluminium, and gold for energies spanning the dynamic range of our PWM cross sections. These results are shown in figs. 1–3.

In a classical interpretation, the difference in the forward direction is related to very small deflections at large distances from the nucleus. The atomic electrons shield the effects of the nucleus from the external electron. Molière's screening function is exponential in character while the more sophisticated PWM

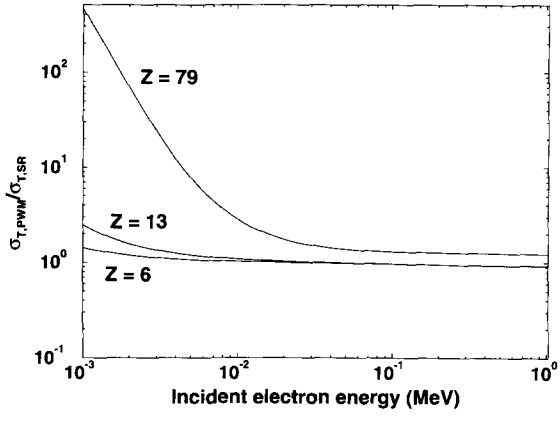


Fig. 5. The ratio of the total transport cross section using the partial-wave method to the screened Rutherford cross section for graphite, aluminium, and gold from 1 to 1024 keV.

employs more realistic electron cloud distributions. Thus, it is not surprising to see large differences at small angles. At large angles the deflections are associated with closer approaches to the nucleus. Differences here have less to do with screening. The screened Rutherford cross section ignores relativistic spin effects which affect the large angle scattering, while the PWM takes these into account.

These differences appear to be very large. Indeed, a comparison of the total cross sections, given in fig. 4, reveals very large differences in total cross section between the PWM and Molière's single scattering cross section with the discrepancy increasing with increased atomic number.

However, it is more relevant to compare the transport cross section [12] defined as $\sigma_T = 2\pi \int_0^\pi \sin\theta \times (1 - \cos\theta)\sigma(\theta)\,d\theta$, which can be interpreted as the amount of scattering per unit length. The transport cross section ratio is depicted in fig. 5. The transport cross section for the PWM is very similar to the screened Rutherford cross section for graphite, aluminium and gold above about 10 keV. Generally, at low energies the PWM predicts more scattering for all materials, more scattering in high-$Z$ materials for all energies, and slightly less scattering at high energies for the low-$Z$ materials shown.

### 3.2. *Multiple scattering distributions*

A user code was written that scored the angular deflection of the electron after a given amount of total curved path length was achieved[#5]. All energy loss processes were turned off to isolate the effects of elastic scattering. Results for graphite are given in figs. 6–8, aluminium in figs. 9–11, and gold in figs. 12–14. Predictions of the Molière theory are given by the solid and dotted smooth lines. The solid curves include Bethe's large-angle correction factor [17], $(\Theta/\sin\Theta)^{1/2}$, while the dotted lines do not include this correction. The Monte Carlo predictions based on the PWM are depicted as solid histograms, while the results obtained using the screened Rutherford cross section are represented as histograms with dashed lines. In each case the Monte Carlo predictions are based on $10^5$ electron histories. The curves were normalised to unity by integration between 0 and $\pi$ with respect to $\sin\Theta\,d\Theta$, where $\Theta$ is the scattering angle.

There are several general features to note. The Molière parameter, $\Omega_0$, can be interpreted roughly as the number of atomic collisions participating in the multiple scattering deflection. The lower bound, below which the analytic expressions break down mathematically, occurs at $\Omega_0 = e$ [6]. It has been argued previously [6] that some sensible results, in particular the estimates of path curvature and lateral deflection during a single transport step, may be obtained by allowing electron step-sizes to be reduced to this mathematical lower bound. Evidence of breakdown of the angular distributions can be observed by the spurious wiggles in the theoretical predictions. Indeed, the mathematical breakdown appears to occur somewhat higher than $\Omega_0 = e$, since the probability distributions are negative for some angular intervals.

Molière considered his theory valid for $\Omega_0 > 20$. For comparison purposes, the $\Omega_0 = 20$ comparisons are also shown. The agreement of the screened Rutherford results with the Bethe-corrected Molière distributions are excellent for all energies. Also shown are the results for at least one step-size intermediate between $\Omega_0 = e$ and $\Omega_0 = 20$ (usually $\Omega_0 = 5$). The spurious structure in the theoretical distributions has nearly disappeared by this point and the comparison with the screened Rutherford single scattering Monte Carlo remains relatively good[#6].

The maximum step-size considered valid for the Molière theory has been stated by Bethe [17] to be such that the average scattering angle be less than one radian. The results for this maximum step-size have been plotted for all energies and materials. The effect of the Bethe large-angle correction is most evident at the maximum step-size and the screened Rutherford single scattering Monte Carlo indicates better agreement with the Bethe-corrected Molière distributions.

In general, the PWM results indicate that the scattering from screened Rutherford cross sections, either in single scattering or multiple scattering, is underestimated in the energy range studied. The difference appears to become greater with increased $Z$. This may have been expected from the earlier comparisons of total and transport cross sections.

Overall, the agreement of the multiple scattering distributions with the screened Rutherford single scattering results confirms the soundness of Molière's theory, particularly in the region $\Omega_0 > 5$. However, there is strong suggestion that the Molière distributions may be improved by considering a more sophisticated single scattering cross section. Apart from elastic scattering differences, it has been suggested previously [6]

[#5] In a single scattering model, curved path and geometric transport steps are the same between two elastic scattering interaction points assuming the inelastic process contribute negligibly to the path curvature.

[#6] The Molière theory is expressed as an expansion in $B^{-1}$; $\Omega_0 = e^B/B$. The conventional expansion includes just three terms. It is tempting to assume that more terms would be more accurate at lower values of $\Omega_0$. However, this just introduces more spurious wiggles in the distribution [18].

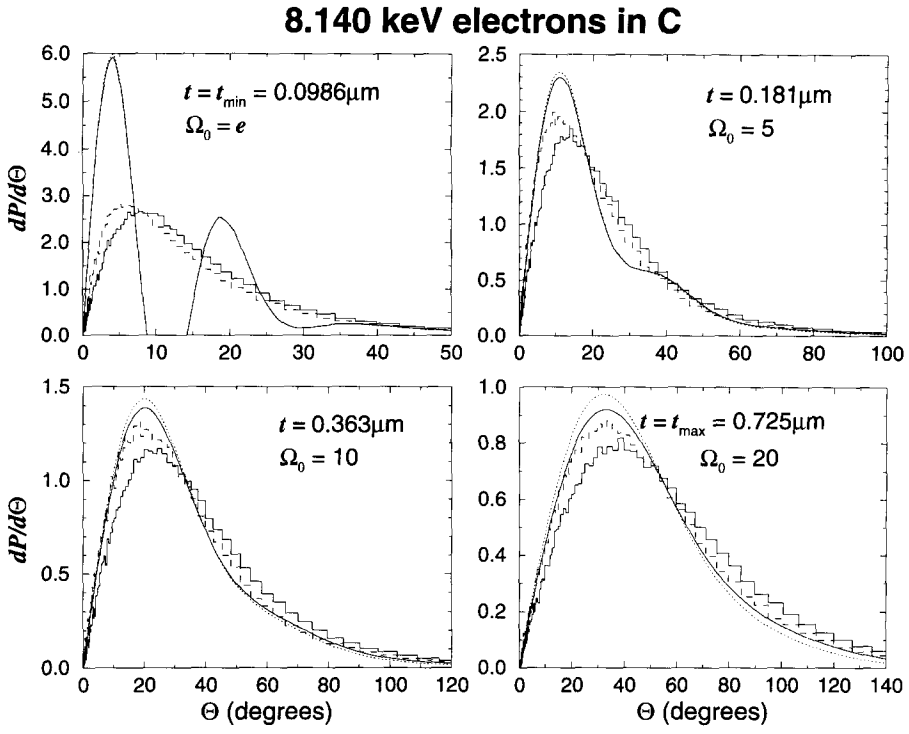


Fig. 6. Multiple scattering angular distributions, $dP/d\Theta$, for 8.140 keV electrons in graphite vs $\Theta$ for total distances ranging from $t$ = 0.0986 $\mu$m ($\Omega_0$ = e, the minimum electron step-size allowed by Molière theory) to $t$ = 0.725 $\mu$m ($\Omega_0$ = 20, the lower physical bound for Molière theory and also the maximum step-size for this energy). The solid curves include Bethe's large-angle correction factor, $(\Theta/\sin\Theta)^{1/2}$, while the dotted curves do not include this correction. The Monte Carlo predictions based on the PWM are depicted as solid histograms, while the results obtained using the screened Rutherford cross section are represented as histograms with dashed lines.

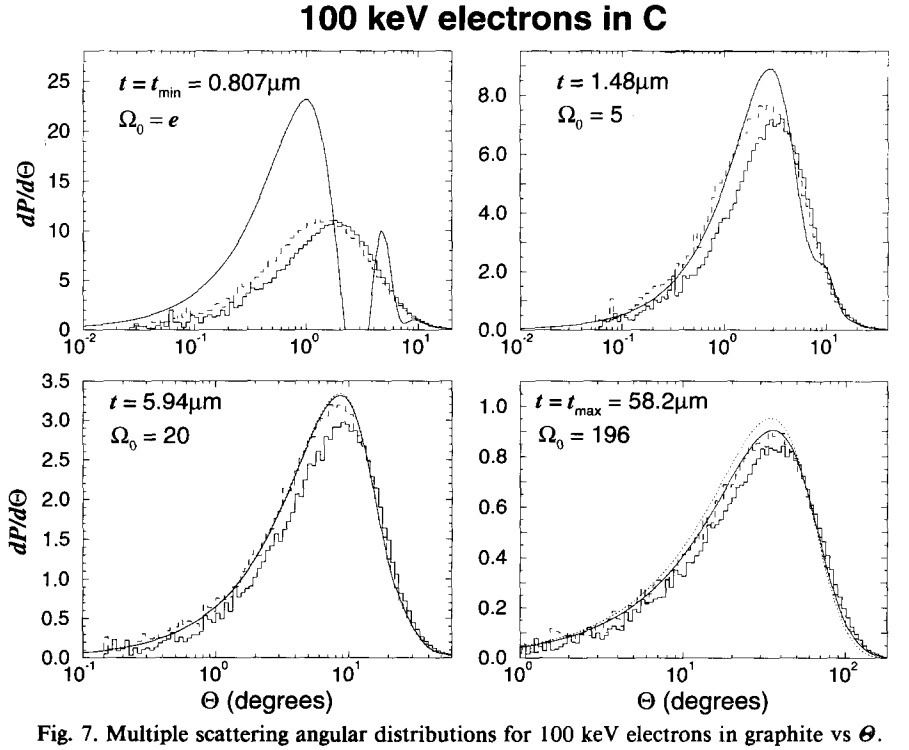


Fig. 7. Multiple scattering angular distributions for 100 keV electrons in graphite vs $\Theta$.

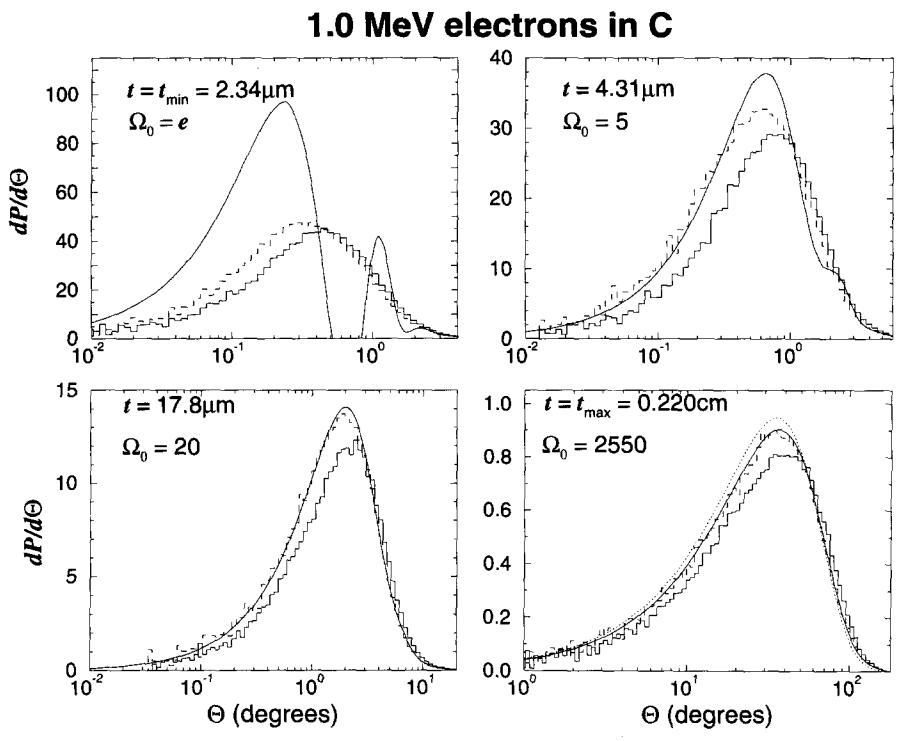


Fig. 8. Multiple scattering angular distributions for 1.0 MeV electrons in graphite vs $\Theta$.

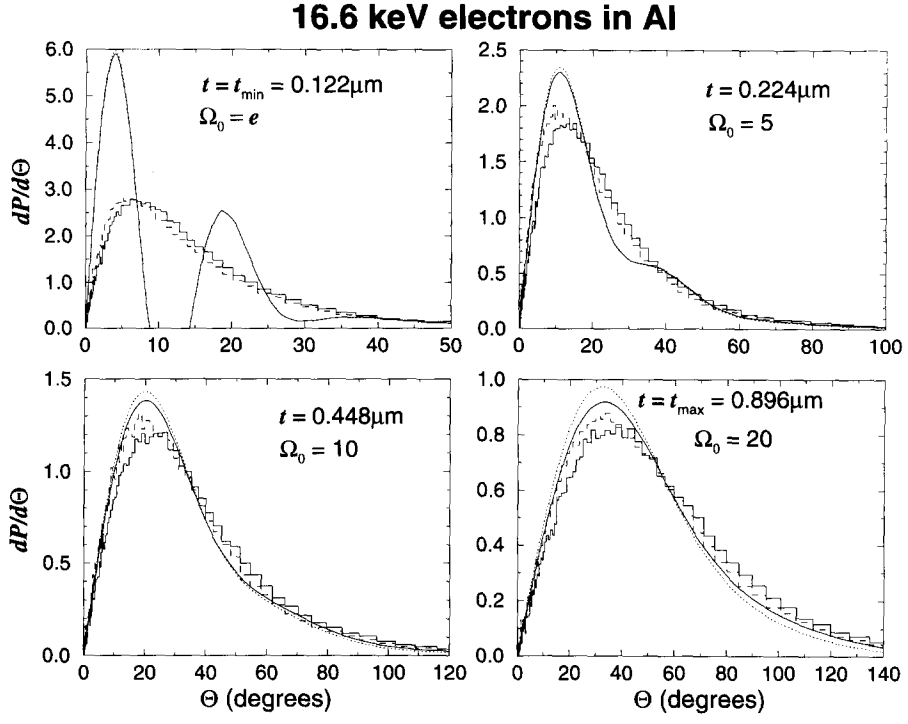


Fig. 9. Multiple scattering angular distributions for 16.6 keV electrons in aluminium vs $\Theta$.

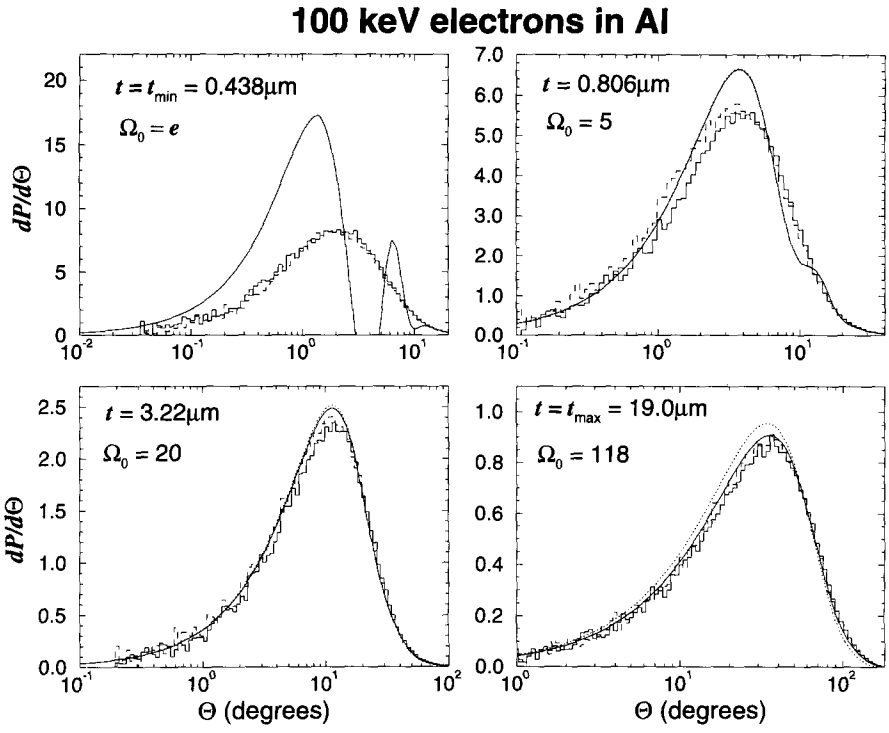


Fig. 10. Multiple scattering angular distributions for 100 keV electrons in aluminium vs $\theta$.

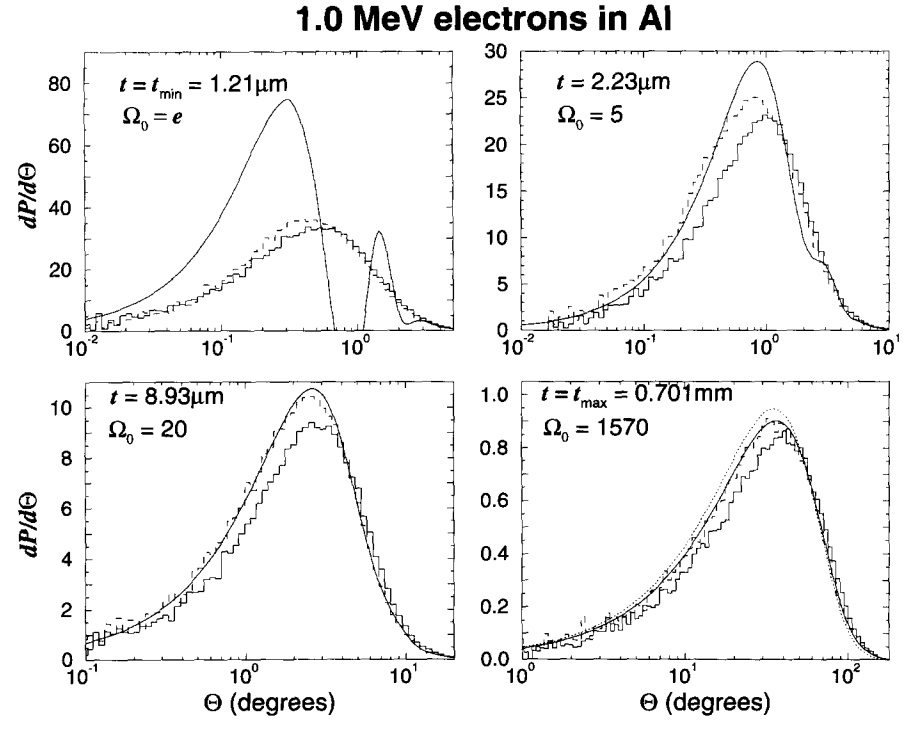


Fig. 11. Multiple scattering angular distributions for 1.0 MeV electrons in aluminium vs $\theta$.

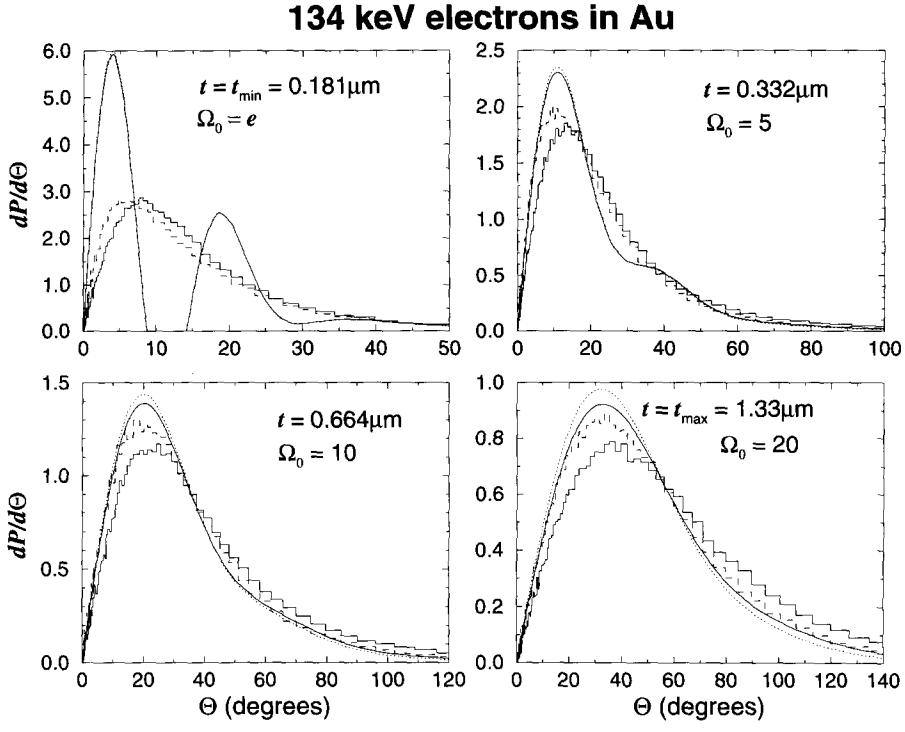


Fig. 12. Multiple scattering angular distributions for 134 keV electrons in gold vs $\Theta$.

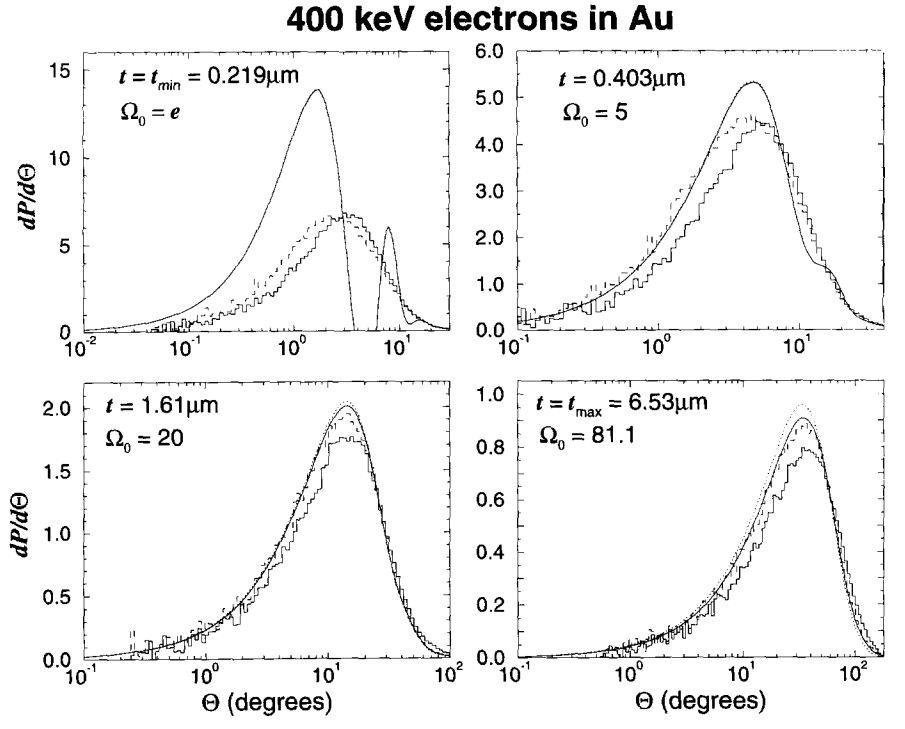


Fig. 13. Multiple scattering angular distributions for 400 keV electrons in gold vs $\Theta$.

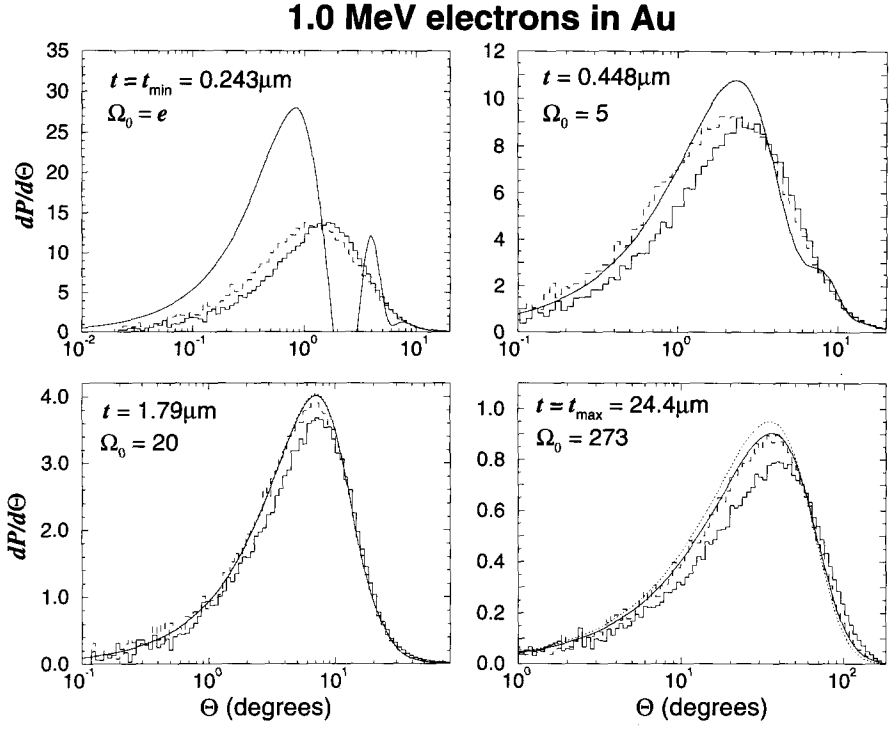


Fig. 14. Multiple scattering angular distributions for 1.0 MeV electrons in gold vs $\Theta$.

that the cause of the backscatter problem in the condensed history technique has to do with the relationship between the total curved path and the position of the particle at the end of the step. If $t$ is the total curved path of the step, the position, $\boldsymbol{x}$, at the end of the step is given by

$$\boldsymbol{x} = \boldsymbol{x}_0 + \boldsymbol{u}_0 s(t) + \boldsymbol{u}_{0,\perp}\, \rho(t), \qquad (1)$$

where $\boldsymbol{x}_0$ is the starting position, $\boldsymbol{u}_0$ is the direction at the beginning of the step, $s(t)$ is the geometrical displacement along $\boldsymbol{u}_0$, and $\rho(t)$ is the lateral displacement along a direction $\boldsymbol{u}_{0,\perp}$ which is orthogonal to $\boldsymbol{u}_0$. Both EGS4/PRESTA [6] and ETRAN/TLC [4] make assumptions about the forms of $s(t)$ and $\rho(t)$ with good but incomplete success. Single scattering methods will allow these distributions to develop without making approximations but at the cost of much more numerical computation.

## 4. Conclusions

Single elastic scattering has been introduced in the EGS4 code. This capability provides a new theoretical laboratory for studying electron transport and the effect of the use of simple cross sections and other approximations. Two single scattering cross sections were introduced. One employed the screened Rutherford cross section upon which the Molière distribution is based. This allowed the verification of the Molière distributions after correction at large angles by Bethe's $(\Theta/\sin\Theta)^{1/2}$ factor. These results demonstrate that the Molière formalism is a successful summation procedure for multiple scattering insofar as the fundamental cross sections allow. Agreement for $\Omega_0 > 20$ is excellent, while lower step-sizes, $5 < \Omega_0 < 20$, may be employed with some compromise in accuracy.

The partial-wave single scattering cross sections are based upon phase-shift data and represent an improved single scattering basis compared to the screened Rutherford cross section employed in EGS4's implementation of the Molière formalism. The results obtained with these cross sections differ from the screened Rutherford results, the differences increasing with increased $Z$. This indicates that Molière theory may be improved by incorporating a better single-scattering cross section.

## Acknowledgements

The authors would like to thank Dr. P. Andreo (Karolinska Institute, Stockholm), Dr. A. Nahum (Royal Marsden Hospital, London), and Dr. D. Rogers (National Research Council, Ottawa) for providing a critique of this manuscript.

## References

[1] W.R. Nelson, D.W.O. Rogers and H. Hirayama, The EGS4 Code System, Stanford Linear Accelerator report SLAC-265 (Stanford, CA, 1985).
[2] J.A. Halbleib and T.A. Mehlhorn, ITS: The Integrated Tiger Series of coupled electron/photon Monte Carlo transport codes, Sandia National Laboratories report SAND84-0573 (1984).
[3] J.S. Hendricks and J.F. Breismeister, IEEE Trans. Nucl. Sci. 39 (1992) 1035.
[4] S.M. Seltzer, Appl. Radiat. Isot. (Int. J. Radiat. Appl. Instrum. Part A) 42 (1991) 917.
[5] M.J. Berger, Meth. Comput. Phys. 1 (1963) 135.
[6] A.F. Bielajew and D.W.O. Rogers, Nucl. Instr. and Meth. B 18 (1987) 165.
[7] C.T. Ballinger, The Response History Monte Carlo method for Electron Transport, Thesis, University of Michigan (1991).
[8] D.E. Cullen, S.T. Perkins, E.F. Plechaty and J.A. Rathkopf, The All Particle Method: Coupled neutron, photon, electron, charged particle Monte Carlo calculations, Report UCRL-98975 (Livermore, CA, 1988).
[9] D.E. Cullen, C.T. Ballinger and S.T. Perkins, The All Particle Method: 1991 Status Report, Report UCRL-JC-108061 (Livermore, CA, 1991).
[10] M.E. Riley, C.J. MacCallum and F. Biggs , At. Data Nucl. Data Tables 15 (1975) 443.
[11] J.P. Desclaux, Comput. Phys. Commun. 9 (1975) 31.
[12] M.J. Berger and R. Wang, Multiple-scattering angular distributions and energy-loss straggling, in: Monte Carlo Transport of Electrons and Photons eds. T.E. Jenkins, W.R. Nelson, A. Rindi, A.E. Nahum and D.W.O. Rogers, (Plenum, New York, 1987) p. 21.
[13] R. Wang, A new scheme for Monte Carlo electron and photon transport, Ph.D. Thesis, Kingston Polytechnic University, Surrey, UK (1993) unpublished.
[14] R. Wang, S. Duane and A.F. Bielajew, A new scheme for Monte Carlo electron and photon transport, NRC Report PIRS-0355.
[15] G.Z. Molière, Z. Naturforsch. 2a (1947) 133.
[16] G.Z. Molière, Z. Naturforsch. 3a (1948) 78.
[17] H.A. Bethe, Phys. Rev. 89 (1953) 1256.
[18] P. Andreo, J. Medin and A.F. Bielajew, submitted to Med. Phys.